# Uplink Cooperative NOMA with Downlink Energy Harvesting in PPP-Based Ultra-Dense Networks

Sinh Cong Lam[1], Quan Vu[2], Duc Tan Tran[3], Nhu-Ngoc Dao[4], Trong Minh Hoang[5]
[1]Faculty of Electronics and Telecommunication, VNU University of Engineering and Technology, Vietnam
[2]Department of Biomedical Engineering, Le Quy Don Technical University, Vietnam
[3]Faculty of Electrical and Electronic Engineering, Phenikaa University, Vietnam
[4]Department of Computer Science and Engineering, Sejong University, South Korea
[5]Telecommunication Faculty No.1, Posts and Telecommunications Institute of Technology, Vietnam

***Abstract*—This paper investigates an uplink cooperative Non-Orthogonal Multiple Access (NOMA) system integrated with energy harvesting in ultra-dense wireless networks, where both base stations (BSs) and users are spatially modeled as independent Poisson Point Processes (PPPs). A distance-dependent cooperative transmission scheme is proposed, allowing a near user to assist a far user only when their separation is below a predefined threshold, thus improving cooperation efficiency and reducing unnecessary relay operations. The near user allocates a fraction $\epsilon$ of its harvested energy to relay the far user's signal, while the remaining $(1-\epsilon)$ portion is used for its own uplink transmission. Using the stretched path loss model and Campbell's theorem, a closed-form expression for the average harvested energy is derived, and system capacity is evaluated through Monte Carlo simulations. Results show that the proposed energy-harvesting cooperative NOMA (EH-C-NOMA) scheme significantly improves network performance, achieving up to 85% higher capacity than the non-cooperative case and 11.63% improvement over full cooperation.**

***Index Terms*—Cooperative NOMA, energy harvesting, stochastic geometry, Poisson point process, ultra-dense networks, uplink transmission, Campbell's theorem, stretched path loss.**

## I. Introduction

The explosive growth of data-intensive applications such as immersive multimedia, industrial automation, and the Internet of Things (IoT) has driven the demand for wireless networks that can simultaneously offer higher data rates, ultra-reliable connectivity, and improved energy efficiency. In the context of sixth-generation (6G) networks and beyond, enabling massive connectivity while maintaining spectral and energy efficiency remains one of the most critical design challenges. To meet these requirements, Non-Orthogonal Multiple Access (NOMA) has emerged as a promising multiple access technique that departs from traditional orthogonal schemes by allowing multiple users to share the same time–frequency resources through power-domain multiplexing [1]. By employing superposition coding at the transmitter and successive interference cancellation (SIC) at the receiver, NOMA effectively improves spectral efficiency and accommodates multiple users concurrently, making it particularly attractive for ultra-dense IoT deployments [2].

Despite its advantages, the practical implementation of NOMA—especially in uplink scenarios—faces several challenges such as multi-user interference, error propagation in the SIC process, and dynamic power allocation among users [3]. Recent research has shown that cooperative communication can serve as an effective means to address these issues by exploiting spatial diversity and improving link reliability through user cooperation or relay assistance. In cooperative NOMA (C-NOMA) systems, a near user can assist a far user by forwarding its signal to the base station (BS), thereby improving the cell-edge user's reception quality. Such cooperation helps overcome severe path loss or blockage, effectively extending network coverage and enhancing fairness across users. A recent survey in [5] provides a comprehensive overview of cooperative NOMA architectures and highlights energy-harvesting-assisted cooperation as a key enabler for sustainable 6G networks. Likewise, the work in [4] and [5] demonstrated that energy-harvesting-based cooperative relaying can sustain network operation while mitigating the power limitations of edge devices.

Energy efficiency remains a fundamental bottleneck for large-scale wireless networks, particularly in IoT scenarios where a vast number of devices are battery-powered and often deployed in remote or hard-to-access areas. Energy harvesting (EH) technologies provide a sustainable solution by enabling wireless nodes to convert ambient energy sources, such as radio-frequency (RF) signals, into usable electrical energy. Among various EH techniques, Simultaneous Wireless Information and Power Transfer (SWIPT) has attracted substantial attention for its ability to allow users to harvest energy and decode information simultaneously from the same RF waveform. Recent experimental and theoretical advances [6], [7] have demonstrated that SWIPT can significantly enhance energy sustainability and reduce operational costs, paving the way for self-powered IoT systems and energy-autonomous communications.

Building upon these concepts, integrating energy harvesting with cooperative NOMA creates a powerful framework for achieving both energy sustainability and spectral efficiency. In energy-harvesting cooperative NOMA (EH-C-NOMA) systems, users or relay nodes can harvest energy from base station transmissions during a dedicated harvesting phase and use this harvested energy to forward information during the transmission phase [1]. This eliminates the need for fixed power supplies and enables self-sustaining operation. Recent studies [8], [9] have also analyzed the outage behavior and capacity limits of EH-assisted NOMA networks with direct and cooperative links, confirming substantial reliability improvements under realistic fading and path loss conditions.

To capture the randomness and spatial heterogeneity of dense network deployments, stochastic geometry has become a standard analytical framework. It enables tractable yet realistic modeling of base station and user distributions by representing their locations as independent Poisson Point Processes (PPPs). Through this framework, several works [10] have derived closed-form expressions for performance metrics such as coverage probability and spectral efficiency in NOMA-based cellular and vehicular networks.

Motivated by the above, this paper investigates an uplink ultra-dense EH-C-NOMA system where both base stations and users are spatially distributed as independent PPPs. The main contributions of this paper are summarized as follows:

- We derive the closed-form expression for the average harvested energy at typical users using Campbell's theorem and the stretched path loss model.
- We propose a distance-dependent cooperative transmission strategy and characterize the cooperation regions based on geometric relationships between near and far users.
- We analyze the system performance under both cooperative and non-cooperative scenarios, providing insights into the impact of network density, energy harvesting efficiency, and cooperation threshold on system performance.

Monte Carlo simulations show that the proposed model significantly enhances system throughput - achieving up to 85% higher capacity than the non-cooperative case and 11.63% improvement compared with full cooperation.

## II. System model

This paper studies an uplink ultra dense network. The location of BSs and users in Euclidean plane are assumed to follow two independent Spatial PPP with intensity of $\lambda_b$ and $\lambda_u$. It is assumed that $\lambda_u >> \lambda_b$ so that there always exists a pair of NOMA users within each cell. Let $P_c$ and $P_e$ as the transmission power of near and far user respectively.

The closest association mechanism is applied so that the user has connection to the nearest BS. The Probability Density Function of the distance $d$ from the typical user to its serving BS is

$$f(d) = 2\pi\lambda d \exp\left(-\pi\lambda d^2\right) \tag{1}$$

Considering a pair of near and far NOMA users whose distance to their serving BSs are $d_1$ and $d_2$ ($d_1 < d_2$). Denote $\phi$ ($0 \leq \phi \leq 2\pi$) as the uniform random variable to represent the angle between two users. Thus, the distance $d_{12}$ between these users are obtained by the cosine law. Specifically,

$$d_{12} = \sqrt{d_1^2 + d_2^2 + 2d_1 d_2 \cos\phi} \tag{2}$$

### A. Channel model

To capture the characteristics of the wireless transmission condition, the Stretched Path Loss model is utilized. Thus, the path loss between transmitter and receiver over a distance of $d$ is $L(d) = \exp\left(-\alpha d^{\beta}\right)$. In practical uplink cellular systems, a user passively receives interference from other users and is therefore unable to estimate the instantaneous channel power gains from these interferers. The work in literature is proved that removing the channel power gains of the interferers from the SIR expression provides a lower bound on user performance. In addition, the channel gain from the serving BS can be approximately estimated using reference signals. Therefore, this paper ignores the instantaneous channel power gain in the performance analysis.

### B. Downlink energy harvesting

During the harvesting phase, the user harvests the energy from the active BSs including both serving and interfering BSs. Assuming that the energy harvesting duration prolongs a time unit and the efficiency of this phase is 1. Let $d_j$ as the distance from the typical user to BS $j$. Thus, the total harvested energy of the typical user is

$$P_e = P_b L(d) + \sum_{j\in\theta_b} P_b L(d_j) \tag{3}$$

where $P_b$ is the BS transmission power, $\theta_j$ is the set of adjacent BSs of the typical user.

*Lemma 2.1:* For a typical user in the proposed system model with the above assumptions, the harvested energy from the BSs is given by

$$P_e = \frac{2\pi\lambda P_b}{\beta}\,\alpha^{-\frac{2}{\beta}}\,\Gamma\left(\frac{2}{\beta}\right) \tag{4}$$

*Proof 2.2:* The harvested energy of the typical user $P_e = \mathbb{E}\left[P_b L(d) + \sum_{j\in\theta_b} P_b L(d_j)\right]$ can be directly computed by applying Campbell's theorem to the homogeneous PPP over the entire plane. Specifically, we have

$$P_e = \lambda P_b \int_{\mathbb{R}^2} e^{-\alpha\|x\|^{\beta}}\,dx. \tag{5}$$

By converting to polar coordinates $(r, \theta)$, the expression becomes

$$P_e = 2\pi\lambda P_b \int_0^{\infty} e^{-\alpha r^{\beta}}\,r\,dr. \tag{6}$$

Employing the change of variables $u = \alpha r^{\beta}$, it follows that

$$r = \left(\frac{u}{\alpha}\right)^{\frac{1}{\beta}}, \quad dr = \frac{1}{\beta}\alpha^{-\frac{1}{\beta}}u^{\frac{1}{\beta}-1}\,du. \tag{7}$$

Substituting into the integral, we obtain

$$\int_0^{\infty} e^{-\alpha r^{\beta}}\,r\,dr = \frac{1}{\beta}\alpha^{-\frac{2}{\beta}}\Gamma\left(\frac{2}{\beta}\right). \tag{8}$$

Finally, the closed-form expression for the average interference is

$$P_e = \frac{2\pi\lambda P_b}{\beta}\,\alpha^{-\frac{2}{\beta}}\,\Gamma\left(\frac{2}{\beta}\right) \tag{9}$$

### C. Uplink Cooperative NOMA

To ensure acceptable performance, the user is allowed to utilize both the harvested energy and the available battery energy for data transmission phase. In addition, the transmission cooperation between near and far users is applied so that the near user receives and forwards the signal of far user to the serving BS. In addition, due to the heavy path loss between over distances, the cooperative transmission only takes place if and only if the distance between two users is smaller than the pre-defined threshold $d_0$, $d_{12} < d_0$. Thus, the far user is assisted by the near user if and only if its distance $d_2$ satisfies the following conditions

$$\begin{cases} d_2 > d_1 \\ d_1^2 + d_2^2 - 2d_1 d_2 \cos\phi < d_0^2 \end{cases} \tag{10}$$

In other words, the cooperative NOMA technique is enable if $d_1$, $d_2$ and $\theta$ are in one of the following regions

$$\begin{cases} R_1 & : d_2 - d_1 \leq d_0 \leq d_1 + d_2, 0 \leq \theta \leq 2\pi \\ R_2 & : d_0 > d_1 + d_2, 0 \leq \theta \leq 2\pi \end{cases} \tag{11}$$

**Desired signal power** Without cooperative transmission, both near and far users fully utilize the harvested energy for data transmission. Thus, their transmission powers are equal to $P_e$. It should be noted that, due to different path losses to the serving BS, the uplink received signal strengths of the near and far users are also different. Therefore, the BS is able to distinguish their signals even though they transmit at the same power level. The received signal power of near user $S_1^{(o)}$ and far user $S_2^{(o)}$ are obtained by

$$S_1^{(o)} = P_e L(d_1) \text{ and } S_2^{(o)} = P_e L(d_2) \tag{12}$$

With cooperative transmission enabled, the BS receives the far user's signal through both the direct link and the auxiliary link from the near user. At the BS, the selection combining technique is utilized to stronger signal for base band processing. In this scheme, the near user allocates a portion of its harvested energy to forward the far user's message, while the remaining energy is used for its own data transmission. Thus, the uplink desired signal power of the far user is given by

$$\begin{cases} S_1^{(w)} = (1-\epsilon) P_e L(d_1) \\ S_2^{(w)} = \max\left(\epsilon P_e L(d_{12}) L(d_1), P_e L(d_2)\right) \end{cases} \tag{13}$$

where $P_e L(d_{12})$ is the signal power of the far user, that is received by the near user.

**Interference power** For both cooperative and non-cooperative transmission scenarios, both near and far users fully transmit harvested energy. For a given user, the total interference from users at adjacent cells is given by

$$I = \sum_{j \in \theta_b} P_e(d_j) L(d_j) \tag{14}$$

Therefore, the uplink SINR of the near user $SINR_1$ and far $SINR_2$ user are given by

- Without cooperative NOMA transmission

$$SINR_1 = \frac{S_1^{(o)}}{I + \sigma^2} \text{ and } SINR_2 = \frac{S_1^{(o)}}{I + \sigma^2} \tag{15}$$

- With cooperative NOMA transmission

$$SINR_1 = \frac{S_1^{(w)}}{I + \sigma^2} \text{ and } SINR_2 = \frac{S_1^{(w)}}{I + \sigma^2} \tag{16}$$

where $\sigma^2$ is the additive Gaussian noise power.

## III. Average User Capacity

To examine the performance of the proposed NOMA cooperative scheme, the average user data rate is utilized. The instantaneous user capacity with uplink $SINR$ on the unit bandwidth is computed by utilizing the Shannon theorem. Particularly,

$$C = \log_2(1 + SINR) \tag{17}$$

For the NOMA system, there are two users on every sub-band. Therefore, the instantaneous capacity on a given sub-band in BS $k$ is

$$C_n^{(k)} = \log_2(1 + SINR_1^{(k)}) + \log_2(1 + SINR_2^{(k)}) \tag{18}$$

Taking over the network, the average capacity on a given sub-band is

$$C_n = \frac{1}{M} \sum_{k \in \theta} \log_2(1 + SINR_1^{(k)}) + \log_2(1 + SINR_2^{(k)})$$

where $M$ is the number of active BSs that transmit on the sub-band of interest.

## IV. Performance Analysis

In this section, we perform the Monte Carlo simulation to examine the performance of the proposed system model and compare with existing ones. The simulation steps are summarized as follows

**Algorithm 1** Cooperative NOMA simulation with energy harvesting

**Require:** BS density $\lambda_b$, user density $\lambda_u$, number of trials $N$, path loss parameters $(\alpha, \beta)$, BS power $P_b$, reference threshold $d_0$

**Ensure:** Average uplink SIR of far users

Initialize Capacity $\leftarrow 0$
**for** $i = 1$ to $N$ **do**
  Generate position of BSs and users as two independent PPPs with intensities $\lambda_b$ and $\lambda_u$
  Assign each user to its nearest BS
  **Energy harvesting phase:**
  For each user, compute harvested energy

$$P_e = P_b L(d) + \sum_{j \in \theta_b} P_b L(d_j)$$

  Select randomly a near - far user pair per BS
  Compute distances $d_1$, $d_2$pair from the select user pair to the serving BS and angle $\phi$ between these users
  Compute inter-user distance $d_{12} = \sqrt{d_1^2 + d_2^2 + 2d_1 d_2 \cos\phi}$
  **if** $d_{12} < d_0$ **then**
    Enable cooperation
    Desired signal power of the far user $S_{12} = P_e L(d_2) + P_e L(d_{12}) L(d_1)$
  **else**
    No cooperation
    Desired signal power of the far user $S_2 = P_e L(d_2)$
  **end if**
  Compute total interference $I = I_n + I_c$ where $I_n$ and $I_c$ are total interference from all selected near and far users at the adjacent BSs
  **if** cooperation enabled **then**
    SIR $\leftarrow \frac{S_{12}}{I}$
  **else**
    SIR $\leftarrow \frac{S_2}{I}$
  **end if**
  Capacity $\leftarrow$ Capacity $+ 2$ log(1+SIR)
**end for**
**return** Average Capacity$/N$

The simulation environment models both BSs and users as independent PPPs deployed in a square area of side length $R_0 = 1000$ m. BS density is $\lambda_b = 10^{-4}$ BS/m$^2$, and UE density is $\lambda_u = 5 \times 10^{-3}$ UE/m$^2$. The number of BSs and UEs follows Poisson distributions with means $\lambda_b(2R_0)^2$ and $\lambda_u(2R_0)^2$, respectively.

### *A. Average User Capacity vs $\beta$*

To evaluate the impact of transmission conditions on network performance, the following parameters are adopted:

- Parameters $\alpha \in \{0.001, 0.01, 0.1\}$ and $\beta \in [0.5, 2.0]$ (step size 0.05) capture varying attenuation strengths and path loss exponents.
- BS transmit power is $P_b = 1.0$ W, and noise power is $\sigma^2 = 10^{-9}$ W. Each BS serves up to two nearest users via nearest-BS association, enabling downlink NOMA pairing, with users harvesting energy from all BSs.
- Cooperative relaying is activated if the inter-user distance is below $d_0 = 50$ m.
- The near user splits power equally between its signal and relaying for the far user, with power allocation $\epsilon = 0.5$.
- SINR accounts for desired signals, inter-cell interference from all BSs, harvested energy effects, and noise.
- Simulations run $N = 50$ Monte Carlo iterations per $(\alpha, \beta)$ pair, averaging capacities over served users to ensure statistical reliability.

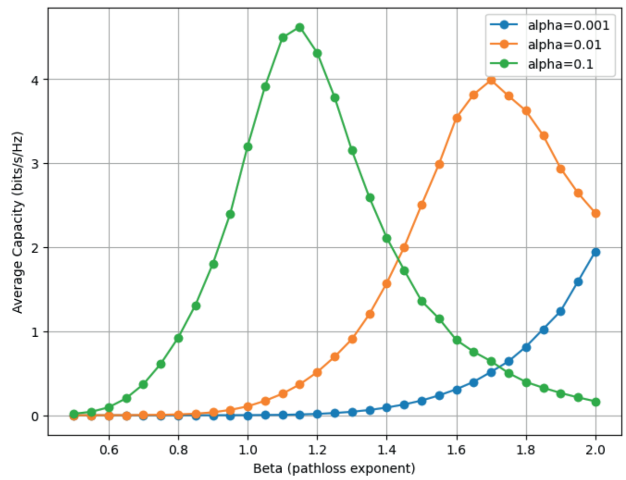


Fig. 1. Average User Capacity vs Path loss parameter $\beta$

Figure 1 depicts the average network capacity (in bits/s/Hz) as a function of the path loss exponent $\beta$, modulated by the attenuation coefficient $\alpha$, within a cooperative Non-Orthogonal Multiple Access (NOMA) network modeled using a Poisson Point Process (PPP). The plotted curves represent $\alpha = 0.001$ (blue), $\alpha = 0.01$ (orange), and $\alpha = 0.1$ (green), with $\beta$ varying from 0.6 to 2.0.

An increase in either $\alpha$ or $\beta$ leads to more severe path loss, thereby intensifying signal attenuation, resulting in increased signal attenuation. This reduction in received power at user terminals diminishes both the desired signal strength and inter-cell interference. Given that capacity is determined by the Signal-to-Interference-plus-Noise Ratio (SINR), the concurrent decline in signal and interference can produce a non-monotonic capacity profile. For $\alpha = 0.1$, capacity reaches a maximum at $\beta \approx 1.4$ (approximately 3.8 bits/s/Hz), indicative of an optimal equilibrium where interference suppression exceeds signal attenuation. In contrast, for $\alpha = 0.001$, capacity increases progressively to 2.0 bits/s/Hz, suggesting that lower attenuation sustains elevated SINR across the $\beta$ spectrum.

These trends are consistent with PPP-based network frameworks, wherein dense deployments intensify interference at lower $\beta$ values, while elevated $\beta$ values (e.g., $\beta > 1.6$)

results in signal attenuation, thereby reducing capacity. Cooperative NOMA, engaged when inter-user distances fall below 50 m, alleviates these effects through relaying; however, its effectiveness wanes under heightened path loss conditions. These findings highlight the critical trade-offs between attenuation parameters and network performance, providing valuable insights for optimizing NOMA implementations in energy-harvesting environments.

### *B. Average Capacity vs Reference distance $d_0$*

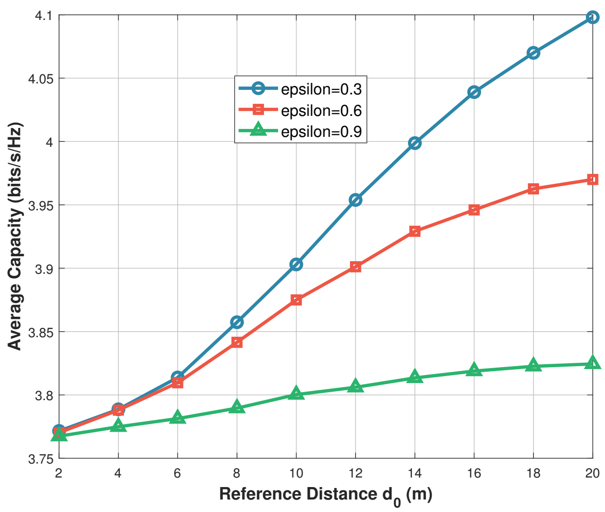


Fig. 2. Average User Capacity vs Reference distance $d_0$

Figure 2 illustrates the variation of the average user capacity with respect to the reference distance for different power allocation factors. As $d_0$ increases, the probability that two users satisfy the cooperation condition $d_{12} < d_0$ also increases. This results in a higher likelihood of cooperative relaying being activated, which strengthens the far user's received signal through the relay-assisted link. Consequently, the average system capacity improves as $d_0$ grows from 2 m to approximately 16 m. Beyond this range, the improvement becomes marginal since almost all user pairs already qualify for cooperation. Notably, the capacity gain is more pronounced for smaller $\epsilon$ values because the near user still retains sufficient power for its own transmission while contributing to the far user's signal.

This behavior confirms the effectiveness of the proposed distance-dependent cooperation mechanism, which adaptively enhances the far user's performance without excessive energy expenditure from the near user.

### *C. Average Capacity vs Power Ratio $\epsilon$*

Figure 3 shows the average capacity as a function of the power allocation coefficient $\epsilon$ for different user densities ($\lambda_u = 3 \times 10^{-3}$, $6 \times 10^{-3}$, and $9 \times 10^{-3}$). When $\epsilon = 0$, no cooperation occurs, and the near user allocates all harvested power for its own uplink transmission. As $\epsilon$ increases, a larger portion of the near user's power is devoted to forwarding the far user's message, which enhances the received signal power of the far user and consequently improves the overall system throughput. However, this improvement comes at the cost of reduced transmit power for the near user. When $\epsilon$ approaches 1, the near user completely sacrifices its own data transmission, leading to a decline in the total system capacity. The proposed cooperative energy-harvesting NOMA scheme achieves the optimal performance at approximately $\epsilon = 0.4$, where the system capacity reaches its maximum value—about 85% higher than the non-cooperative case ($\epsilon = 0$) and 11.63% higher than the full-cooperation case ($\epsilon = 1$). These results reveal that partial cooperative power allocation yields the best trade-off between throughput and fairness, validating the effectiveness of the proposed energy-harvesting C-NOMA framework in ultra-dense networks.

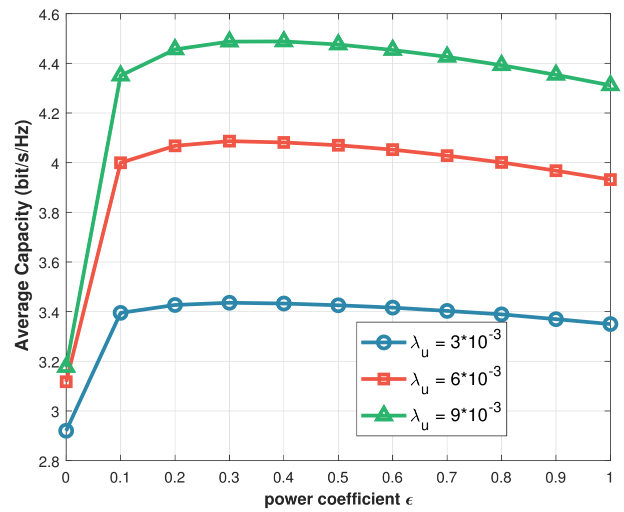


Fig. 3. Average User Capacity vs Power Ratio $\epsilon$

## V. Conclusion

This paper investigated an uplink cooperative NOMA system integrated with energy harvesting in ultra-dense networks modeled by stochastic geometry. By employing the stretched path loss model and Campbell's theorem, a closed-form expression for the average harvested energy was derived. A distance-dependent cooperative transmission strategy was then proposed, enabling near users to assist far users only when their separation is below a predefined threshold. Simulation results demonstrated that this approach significantly enhances system throughput by balancing cooperation benefits and energy efficiency. Specifically, the proposed scheme achieves up to 85% capacity improvement compared with the non-cooperative case ($\epsilon = 0$) and 11.63% higher capacity than full cooperation ($\epsilon = 1$), confirming that partial power allocation ($\epsilon \approx 0.4$) provides the optimal trade-off between user fairness and spectral efficiency. These findings highlight the potential of integrating energy harvesting and distance-based cooperation to improve performance in next-generation dense wireless networks.

# References


[1] Y. Zhou, Y. Zhang, A. A. Khuwaja, Z. Wang, and Q. Zhang, "Analysis of the outage performance of energy-harvesting cooperative-NOMA system with relay selection methods," *Scientific Reports*, vol. 14, no. 10732, May 2024.

[2] V. Andiappan and V. Ponnusamy, "Deep learning enhanced NOMA system: A survey on future scope and challenges," *Wireless Personal Communications*, vol. 123, pp. 1–39, 2022.

[3] V. Ozduran and N. Nomikos, "Performance analysis of inverse successive interference cancellation in NOMA-based communications," *Wireless Networks*, vol. 30, no. 3, pp. 1893–1907, February 2024.

[4] M. Alkhawatrah, "Energy-harvesting cooperative NOMA in IOT networks," *Modelling and Simulation in Engineering*, vol. 2024, p. 1043973, June 2024.

[5] O. Alamu, T. O. Olwal, and K. Djouani, "Cooperative noma networks with simultaneous wireless information and power transfer: An overview and outlook," *Alexandria Engineering Journal*, vol. 71, pp. 413–438, 2023. [Online]. Available: https://www.sciencedirect.com/science/article/pii/S1110016823002302

[6] X. Zhao *et al.*, "High-performance cost efficient simultaneous wireless information and power transfers deploying jointly modulated amplifying programmable metasurface," *Nature Communications*, vol. 14, p. 5883, September 2023.

[7] D. H. Thuan, N.-T. Nguyen, X. T. Nguyen, N. T. Hau, B. V. Minh, and T. N. Nguyen, "Uplink and downlink of energy harvesting noma system: performance analysis," *Journal of Information and Telecommunication*, vol. 8, no. 1, pp. 92–107, 2024.

[8] Y. K. Huang *et al.*, "Outage probability of energy harvesting cooperative NOMA network with direct link," *Journal of King Saud University - Computer and Information Sciences*, July 2025.

[9] T. Z. H. Ernest, A. S. Madhukumar, R. P. Sirigina, and A. K. Krishna, "Capacity characterization of uplink noma in multi-uav networks," in *2020 IEEE 91st Vehicular Technology Conference (VTC2020-Spring)*, 2020, pp. 1–5.

[10] Y. Sun, Z. Ding, X. Dai, M. Zhou, and Z. Ding, "Stochastic geometry based modeling and analysis on network noma in downlink comp systems," *IEEE Transactions on Vehicular Technology*, vol. 73, no. 1, pp. 1388–1393, 2024.